Theoretical investigation of frequency characteristics of free oscillation and injection-locked magnetrons*

Song Yue(岳松)[1,2,†], Dong-ping Gao(高冬平)[1], Zhao-chuan Zhang(张兆传)[1], and Wei-long Wang(王韦龙)[1,2]

[1] *Key Laboratory of High Power Microwave Sources and Technology, Institute of Electronics, Chinese Academy of Sciences, Beijing* 100190, *China*
[2] *University of Chinese Academy of Sciences, Beijing* 100049, *China*

(Received 24 May 2016; revised manuscript received 10 July 2016; published online 28 September 2016)

The frequency characteristics of free oscillation magnetron (FOM) and injection-locked magnetron (ILM) are theoretically investigated. By using the equal power voltage obtained from the experiment data, expressions of the frequency and radio frequency (RF) voltage of FOM and ILM, as well as the locking bandwidth, on the anode voltage and magnetic field are derived. With the increase of the anode voltage and the decrease of the magnetic field, the power and its growth rate increase, while the frequency increases and its growth rate decreases. The theoretical frequency and power of FOM agree with the particle-in-cell (PIC) simulation results. Besides, the theoretical trends of the power and frequency with the anode voltage and magnetic field are consistent with the experimental results, which verifies the accuracy of the theory. The theory provides a novel calculation method of frequency characteristics. It can approximately analyze the power and frequency of both FOM and ILM, which promotes the industrial applications of magnetron and microwave energy.

Keywords: frequency, free oscillation magnetron, injection-locked magnetron, locking bandwidth

PACS: 84.40.Fe, 42.25.Kb, 52.65.Rr **DOI:** 10.1088/1674-1056/25/11/118403

1. Introduction

A magnetron has the advantages of low cost, high efficiency, and high power, so it becomes the preferred microwave source of industrial applications.[1] An injection-locked magnetron (ILM) is the precondition of coherent power combining, which has become the focus of theory, simulation, and experiment studies in the industrial microwave applications.[2–9] The frequency characteristic is the most important aspect of a magnetron, which can reflect the relationship between the radio frequency (RF) voltage, frequency, injection ratio, and the bandwidth with anode voltage and magnetic field. The frequency characteristics of the magnetron mainly consist of two parts: one is the frequency pulling caused by the load changes, and the other is the frequency pushing caused by the anode current.[10] Since the injection signal plays the role of modulation in ILM,[8,9] its frequency characteristic mainly depends on the free oscillation magnetron (FOM). So it is necessary to research the RF voltage and frequency of both FOM and ILM.

The magnetron is affected by many factors, such as orthogonal electric and magnetic fields, as well as the RF field. As it is very difficult to give analytical expressions of electronic admittance and solutions of magnetron self-consistent field equations, many approximation methods and experiments are often adopted to study magnetron.[11–20] Slater gave approximate electron admittance expressions, which are widely used in latter investigations.[11,12] Welch proposed the expression of a frequent pushing parameter on the voltage by studying the formation of electronic spokes, so the frequency pushing parameter can be quantified.[13] For ILM, David presented the expressions of RF voltage and frequency by using an equivalent circuit method, which is widely adopted and developed.[14,15] Woo obtained the time-domain amplitude and phase differential equations of high power ILM power, and performed a dual magnetron mutual-injection-locking experiment.[16] Chen gave the steady-state expressions of RF voltage and frequency of ILM.[17] In recent years, Tahir analyzed the modulation mechanism of the injection signal on the frequency and phase of the magnetron.[18,19]

Despite the fact that the ILM theory has been gradually developed, the existing theories mainly focus on frequency pulling caused by the injection signal, in which the anode voltage and the magnetic field are constant. But in practical applications, the output power of the magnetron is usually adjusted by the voltage or magnetic field, and the oscillation frequency also changes, which has an important impact on both FOM and ILM. However, the present equivalent circuit theory[14,15,17] has not been combined with the frequency pushing theory.[13] So the frequency characteristic of the magnetron with frequency pushing cannot be theoretically calculated with its anode voltage and magnetic field. Especially, the conventional theory cannot solve the variation of the output power and frequency with the magnetic field. Therefore, it is essential to give approximate expressions of frequency and other parameters depending on the anode voltage and magnetic field. The numerical calculation of the theory and the corresponding sim-

*Project supported by the National Basic Research Program of China (Grant No. 2013CB328901) and the National Natural Science Foundation of China (Grant No. 11305177).

†Corresponding author. E-mail: yuessd@163.com

© 2016 Chinese Physical Society and IOP Publishing Ltd

ulation and experimental verification are also indispensable.

This paper is organized as follows. In Section 2, the expressions of the RF voltage and frequency of FOM, as well as the locking bandwidth of ILM, on the anode voltage and magnetic field are obtained by an equivalent circuit method. In Section 3, by numerical calculation, the influences of the anode voltage and magnetic field on the RF voltage, frequency, pushing parameter, and locking bandwidth are analyzed. In Section 4, three-dimensional particle-in-cell (PIC) simulation and experimental measurement are carried out to verify the results of the numerical calculations. Finally, some conclusions are drawn from the present investigation in Section 5.

2. Theoretical analysis

The equivalent circuit model of a magnetron is shown in Fig. 1,[14,15] where g and G represent the conductance of electron and the load, respectively; b and B are the susceptance of electron and the load; and C, R, and L are the equivalent capacitance, resistance, and inductance of the resonant cavity, respectively. The following symbols of frequency will be used: ω_0, the resonant angular frequency of the magnetron; ω', the oscillating angular frequency of FOM; ω_1, the angular frequency of the injected signal; ω, the instantaneous angular frequency of the magnetron; while f_0, f', f_1, and f are the corresponding frequencies.

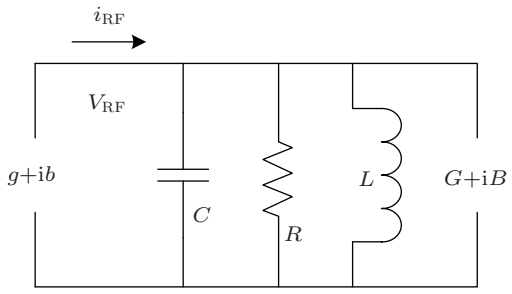


Fig. 1. Equivalent circuit of the magnetron.

When ω' is close to ω_0, the resonator's admittance is $Y(\omega) = 1/R + 2\mathrm{j}C(\omega' - \omega_0)$, where $\omega_0 = 1/\sqrt{LC}$.

The oscillation circuit equation is[16]

$$\frac{g+\mathrm{i}b}{\omega_0 C} = \frac{1}{Q_0} + \mathrm{i}\left(\frac{\omega}{\omega_0} - \frac{\omega_0}{\omega}\right) + \frac{G+\mathrm{i}B}{Q_\mathrm{e}}, \tag{1}$$

where $Q_0 = RC\omega_0$ and Q_e is the external quality factor.

The real and imaginary parts of Eq. (1) represent the stability conditions of amplitude and frequency, respectively, which can be written as

$$\frac{g}{\omega_0 C} = \frac{1}{Q_0} + \frac{G}{Q_\mathrm{e}}, \tag{2}$$

$$\frac{b}{\omega_0 C} = \frac{\omega}{\omega_0} - \frac{\omega_0}{\omega} + \frac{B}{Q_\mathrm{e}}. \tag{3}$$

When the magnetic field is constant, the approximate expression of the electron conductance given by Slater[13] is

$$g = \frac{1}{R}\left(\frac{V_\mathrm{a}}{V_\mathrm{RF}} - 1\right), \tag{4}$$

where V_a is the anode voltage and V_RF is the RF voltage. It should be noted that equation (4) cannot solve the changeable magnetic field problem.

For simplified analysis, we assume that the DC energy of the electrons completely converts to the microwave energy and kinetic energy of the electrons. The energy relation can be written as

$$eV_\mathrm{a} = W + \frac{1}{2}mv^2, \tag{5}$$

where W is the microwave energy and v is the synchronous speed of the electron. For a given magnetic field B_T, the kinetic energy of the electron is provided by the threshold voltage V_t, so there is

$$eV_\mathrm{a} = W + eV_\mathrm{t}. \tag{6}$$

For a different magnetic field, if the microwave energy is constant, the DC voltage and the synchronous speed should change accordingly. When the new DC voltage and magnetic field are V_n and B_n, respectively, in order to ensure constant power is obtained in the same time, there is

$$eV_\mathrm{n} = W + eV_\mathrm{t,n}. \tag{7}$$

Subtracting Eq. (7) with Eq. (6) yields

$$\Delta V_\mathrm{a} = \Delta V_\mathrm{t}. \tag{8}$$

For the magnetron, the threshold voltage satisfies[21]

$$\frac{V_\mathrm{t}}{V_0} = 2\frac{B_\mathrm{T}}{B_0} - 1, \tag{9}$$

where V_0 and B_0 are the synchronous voltage and the magnetic field, respectively, which are determined by the structure dimensions of the magnetron. Thus,

$$\frac{\Delta V_\mathrm{t}}{V_0} = 2\frac{\Delta B}{B_0}. \tag{10}$$

So it can be written as

$$\frac{\Delta V_\mathrm{a}}{\Delta B} = 2\frac{V_0}{B_0}. \tag{11}$$

For equal power magnetrons, the voltage and magnetic field should satisfy

$$V_\mathrm{a} = 2\frac{V_0}{B_0}B_\mathrm{T} + k. \tag{12}$$

The coefficient k should be associated with V_0, B_0, and the power. This value is smaller than the DC voltage. In order

to simplify the analysis, the coefficient k is ignored. So when the power is constant, the anode voltage is approximately proportional to the magnetic field.

According to Varian's experimental data,[10] the equal power lines of the common magnetron are drawn in Fig. 2. As shown in Fig. 2, when the power is constant, the anode voltage is approximately proportional to the magnetic field, which is consistent with the theoretical analysis.

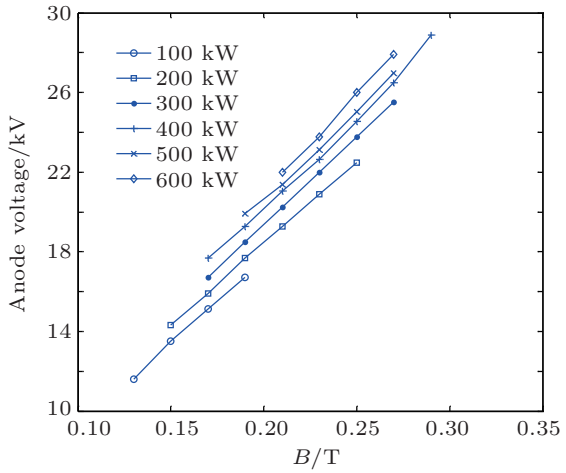


Fig. 2. (color online) Equal power lines of the magnetron.

If the anode voltage V_a is constant and the magnetic field changes from B_1 to B_T, the new working point's magnetic field is B_T and the anode voltage is V_{a1}. So the equal power anode voltage V_{ae} for B_1 should be

$$V_{ae} = V_a \frac{B_1}{B_T}. \tag{13}$$

Substituting Eq. (13) into Eq. (4), we can obtain the expression of electron conductance with different anode voltages and magnetic fields

$$g = \frac{1}{R}\left(\frac{V_a}{V_{RF}}\frac{B_1}{B_T} - 1\right). \tag{14}$$

The approximate electron susceptance of the magnetron is given by[15]

$$b = b_0 - g\tan\alpha, \tag{15}$$

where b_0 is a constant, which is difficult to obtain from experiments, but it has rarely any effect on the frequency; α is the frequency pushing parameter to research, which represents the phase difference between the RF field and the electron spokes. Slater proposed that the electron admittance function on conductance has a negative slope,[13] so $\tan\alpha$ is positive.

The magnetron's working voltage V_a should be within the limited range between its threshold voltage V_t and the cutoff voltage V_C. According to the motion of electrons and the space charge theory, the expressions of V_t and V_C can be given by

$$V_t = \frac{r_a^2}{2}\left(1 - \frac{r_c^2}{r_a^2}\right)\frac{\omega}{n}B_T - \frac{r_a^2}{2}\frac{m}{e}\left(\frac{\omega}{n}\right)^2, \tag{16}$$

$$V_C = \frac{e}{8m}r_a^2\left(1 - \frac{r_c^2}{r_a^2}\right)^2 B_T^2, \tag{17}$$

where r_a and r_c are the anode radius and the cathode radius, respectively, ω is the angular frequency, and n is the mode number. For the π mode, n is half of the cavity number of the magnetron. m and e are the mass and the charge of the electron, respectively.

According to the formation mechanism of space charge spokes, the approximate relationship between α and the anode voltage and the RF voltage can be expressed as[13]

$$\cos 2\alpha = \frac{V_a - V_t}{V_{RF}}. \tag{18}$$

To correspond with the electronic admittance, α should be positive, which can be written as

$$\alpha = \frac{1}{2}\arccos\frac{V_a - V_t}{V_{RF}}, \tag{19}$$

$$\cos\alpha = \sqrt{\frac{V_a - V_t + V_{RF}}{2V_{RF}}}. \tag{20}$$

Substituting Eqs. (13)–(15) and (19) into Eqs. (2) and (3) yields the steady-state RF voltage and frequency of free oscillation magnetron, which can be written as

$$V_{RF0} = \frac{1}{2\gamma}\frac{V_a}{RC}\frac{B_1}{B_T}, \tag{21}$$

$$\omega' = \omega_0 + \frac{1}{2}\left(\frac{b_0}{C} - \frac{B\omega_0}{Q_e}\right) - \frac{\omega_0}{2Q_L} \times \tan\left(\frac{1}{2}\arccos\frac{V_aB_1 - V_tB_T}{\frac{1}{2\gamma}\frac{V_aB_1}{RC}}\right), \tag{22}$$

where γ is the increasing parameter whose value is $\omega_0(1/Q_L + 1/RC\omega_0)/2$, and Q_L is the load quality factor, $1/Q_L = 1/Q_0 + G/Q_e$. Via Eqs. (21) and (22), the influence of the anode voltage and magnetic field on the RF voltage and frequency of FOM can be analyzed.

An actual injection-locked system diagram is shown in Fig. 3. The corresponding equivalent circuit model is shown in Fig. 4. In Fig. 4, g' and b' represent the conductance and the susceptance of the electron, respectively. Similarly, G' and B' represent the conductance and the susceptance of the injection source, respectively.

The injection signal with angular frequency ω_1 ($\omega_1 \approx \omega_0$), voltage V_1, and current I_1 is injected into the magnetron after two circulators. So the load admittance of the magnetron is divided into two parts, one is the actual load and the other is the injection signal. The reflection signal by the load can be absorbed. Therefore, the loading effect of the injection signal plays the main role.

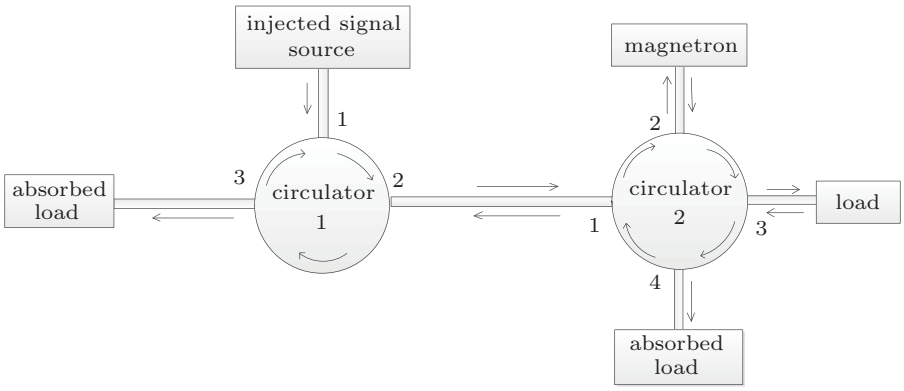


Fig. 3. ILM system diagram.

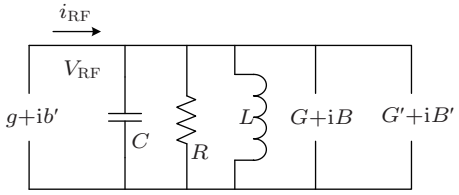


Fig. 4. Equivalent circuit of ILM.

Since G is normalized, the injection ratio can be expressed as $\rho = V_1/(V_{RF0}+V_1)$. When V_{RF0} is small, V_1 is not negligible compared to V_{RF0}. For ILM, the oscillation circuit equation becomes

$$\frac{g'+\mathrm{i}b'}{\omega_0 C} = \frac{1}{Q_0} + \mathrm{i}\left(\frac{\omega}{\omega_0} - \frac{\omega_0}{\omega}\right) + \frac{G+\mathrm{i}B+G'+\mathrm{i}B'}{Q_e}, \quad (23)$$

where $G'+\mathrm{j}B' = 2\rho\,\mathrm{e}^{-\mathrm{j}\theta}$.

Then the new stability conditions can be written as[17]

$$\frac{g'}{c\omega_0} = \frac{1}{Q_L} + \frac{2\rho\cos\theta}{Q_e}, \quad (24)$$

$$\frac{b'}{c\omega_0} = \frac{2(\omega-\omega_0)}{\omega_0} + \frac{B}{Q_e} - \frac{2\rho\sin\theta}{Q_e}, \quad (25)$$

where θ is the phase difference between the injection signal and the output signal.

Similarly, the RF voltage and the operating frequency of ILM can be obtained as

$$V_{RF} = \frac{1}{2\gamma}\frac{V_a}{RC}\frac{B_1}{B_T}\frac{1}{1+\dfrac{\rho\omega_0\cos\theta}{Q_e\gamma}}, \quad (26)$$

$$\omega - \omega' = \frac{\omega_0\rho}{Q_e\cos\alpha}\sin(\theta-\alpha). \quad (27)$$

The angular frequency difference between the injection signal frequency and the free oscillation frequency is $\Delta\omega = |\omega_1 - \omega'|$, while Δf is the corresponding frequency difference. The frequency difference is the biggest during the injection-locking progress. Only if $\Delta\omega$ meets the trigonometric condition (27), the magnetron can be injection-locked. Then, the locking range is

$$\Delta\omega \le \frac{\omega_0\rho}{Q_e\cos\alpha}. \quad (28)$$

The upper limit of the range is defined as the locking bandwidth, namely,

$$\text{bandwidth} = \frac{\omega_0\rho}{Q_e\sqrt{\dfrac{V_a - V_t + V_{RF0}}{2V_{RF0}}}}. \quad (29)$$

From Eqs. (26) and (29), the influence of the anode voltage and magnetic field on the RF voltage and locking bandwidth of ILM can be analyzed. Equation (29) shows that when considering the frequency pushing effect, the locking bandwidth is wider than that of the Adler theory.

In addition, similar to the case without frequency pushing, the steady-state phase difference is independent of the initial value, which can be expressed as

$$\theta = \arcsin\frac{\Delta\omega Q_e\cos\alpha}{\omega_0\rho} + \alpha. \quad (30)$$

When the injection power and frequency are constant, the frequency difference Δf and the locking bandwidth will change with the anode voltage and magnetic field, which may cause the failure of the injection-locked system. Therefore, it is necessary to analyze the relation between Δf, locking bandwidth, and anode voltage or magnetic field.

3. Numerical calculation

A six-cavity magnetron is taken as an example, whose r_a and r_c are 15.56 mm and 4.89 mm, respectively. To simplify the calculations, the load is assumed to be well matched, so $B = 0$. Eigenmode simulation of the magnetron shows $f_0 = 940$ MHz, $Q_e = 150$, and $Q_0 = 2630$. Then it can be inferred that $Q_L = 141.91$, $C = 2.54\times10^{-8}$ F, $g = 1.057$ S, and $R = 17.53\ \Omega$. b_0 has less impact on the result, so its value is set to be 0.1 S.

The threshold voltage and cutoff voltage of the magnetron are shown in Fig. 5. Meanwhile, to ensure that equation (18) is reasonable, V_a cannot be too large. Therefore, the working range is determined by the threshold voltage and the limits of Eq. (18).

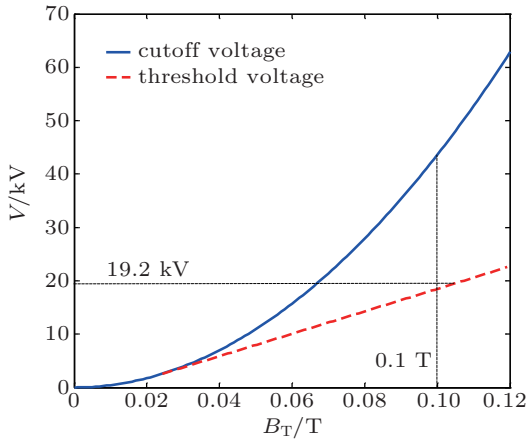


Fig. 5. (color online) The relation between the anode voltage and the magnetic field of the magnetron.

When the magnetic field $B_T = 0.1$ T, the threshold voltage is 18.8 kV. The relationship between the RF voltage and the anode voltage of FOM can be obtained from Eq. (21). According to the simulation, the port voltage is nearly 18.5% of the RF voltage. Then the output power can be obtained by

$$P_{out} = 0.5G_L(0.185V_{RF0})^2. \quad (31)$$

The effect of the anode voltage on the RF voltage and power of FOM is shown in Fig. 6. The change tendency of the frequency and pushing parameter of FOM with the anode voltage can be obtained from Eqs. (22) and (19), as shown in Fig. 7.

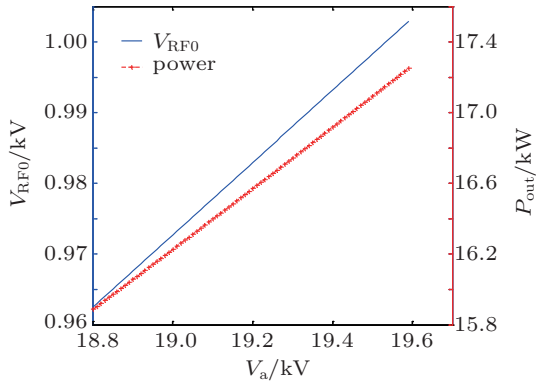


Fig. 6. (color online) Effect of the anode voltage on the RF voltage and power of FOM.

Figure 6 shows that the RF voltage increases linearly with the anode voltage, and the power shows a quadratic growth with the anode voltage. According to Eq. (21), V_{RF0} is proportional to V_a. So P_{out} is a quadratic function of V_a, and the growth rate increases with the increasing V_a. In order to meet the trigonometric function in Eq. (18), the ranges of V_a and B_T are limited. So in this range, the quadratic trend of the power with V_a in Fig. 6 is inconspicuous.

As seen in Fig. 7, with the increase of the anode voltage, the frequency pushing effect gradually decreases and the frequency increases. The frequency pushing reduces the frequency. It should be noted that, due to the presence of the electron admittance and frequency pushing, the oscillation frequency is always lower than the resonant frequency.

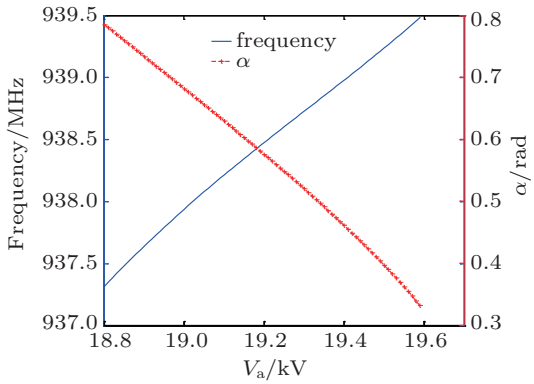


Fig. 7. (color online) Effect of the anode voltage on the frequency and pushing parameter of FOM.

Furthermore, the other way to increase the power is to lower the magnetic field. When the anode voltage is 19.2 kV, the parameters of the magnetron are researched with varied magnetic field from 0.099 T to 0.106 T.

The change tendency of the RF voltage and output power of FOM with the magnetic field can be given by Eq. (21), as shown in Fig. 8. The change tendency of the frequency and pushing parameter of FOM with the magnetic field is shown in Fig. 9, which is obtained from Eqs. (22) and (19).

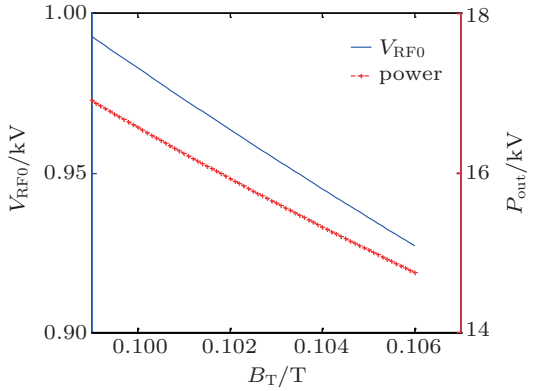


Fig. 8. (color online) Effect of the magnetic field on the RF voltage and power of FOM.

According to Eq. (21), V_{RF0} is an inverse function of the magnetic field. Therefore, the power increases with the decreasing magnetic field and the growth rate increases. Due to the parameters we selected, the range of the magnetic field is limited, so the quadratic relation in Fig. 8 is not obvious.

As seen from Figs. 8 and 9, when the magnetic field reduces, the equivalent anode voltage increases, so that the RF voltage and the resonant frequency increase, while the frequency pushing weakens. Therefore, the influence of the magnetic field on the RF voltage and frequency resonance is consistent with the anode voltage.

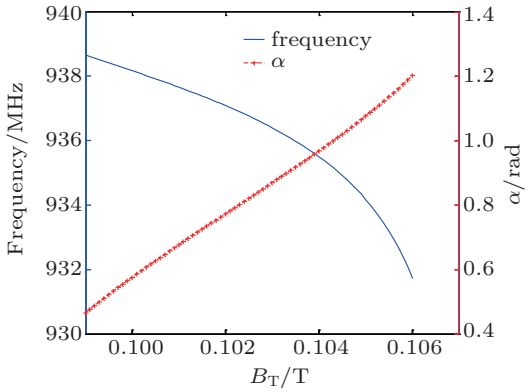


Fig. 9. (color online) Effect of the magnetic field on the frequency and pushing parameter of FOM.

For ILM, the effects of the anode voltage or magnetic field on the RF voltage and locked bandwidth are also analyzed. When $f_1 = 938$ MHz and $B_T = 0.1$ T, trends of the frequency difference and locking bandwidth of ILM with the anode voltage are shown in Fig. 10, in which the injection voltage is set to be 100 V, 200 V, and 300 V respectively.

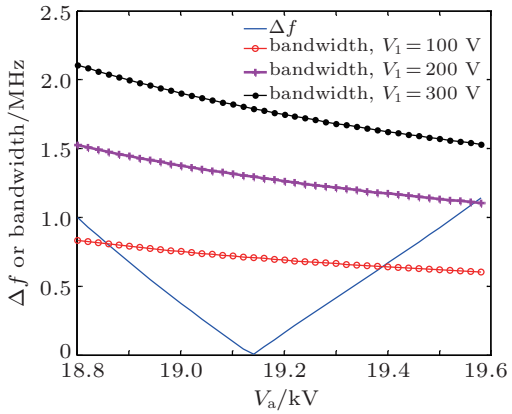


Fig. 10. (color online) Effect of the anode voltage on the frequency difference and locking bandwidth of ILM.

As shown in Fig. 10, with the increase of the anode voltage, the locking bandwidth decreases, and the frequency increases. Therefore, the frequency difference decreases firstly, and then increases. However, when the voltage continues to increase, the frequency difference may be larger than the locking bandwidth, which would lead to the failure of locking. Higher injection power can increase the locking bandwidth, so it increases the anode voltage range.

When $V_1 = 300$ V, $f_1 = 938$ MHz, and $B_T = 0.1$ T, trends of the RF voltage and injection ratio with the anode voltage of ILM can be given by Eq. (25), as shown in Fig. 11.

As can be seen from Fig. 11, when the voltage is near the threshold voltage, the RF voltage is small and the injection ratio is large. With the increase of the anode voltage, the injection ratio decreases. In addition, the RF voltage of ILM is usually smaller than that of FOM.

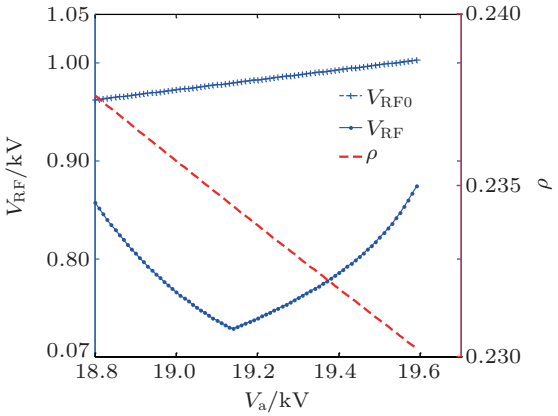


Fig. 11. (color online) Effect of the anode voltage on the RF voltage and injection ratio of ILM.

With the parameters we chose, when $V_a = 19.15$ kV, the frequency of the injection signal is very close to the frequency of FOM. At this time, the steady-state phase difference has the minimum value. And the equivalent conductance of the injection signal G' has the maximum value. With the increase of V_a, the frequency of FOM increases and $\Delta\omega$ decreases. The load effect of the injection signal enhances, so V_{RF} first decreases. With further increase of V_a, the frequency of FOM and $\Delta\omega$ increase. Then the load effect of the injected signal weakens, V_{RF} gradually increases.

Similarly, when $f_1 = 938$ MHz and $V_a = 19.2$ kV, trends of the frequency difference and locking bandwidth with the magnetic field are shown in Fig. 12. Trends of the RF voltage and injection ratio with the magnetic field of ILM are shown in Fig. 13 when $V_1 = 300$ V.

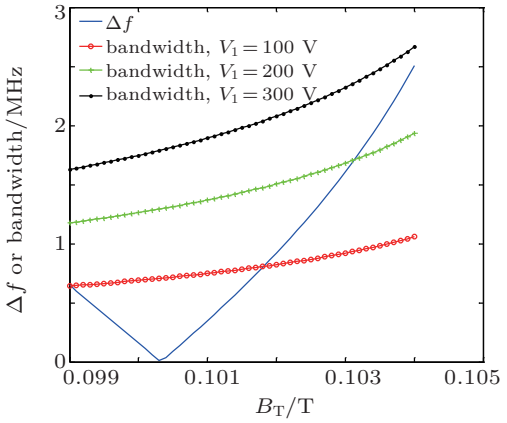


Fig. 12. (color online) Effect of the magnetic field on the frequency difference and locking bandwidth of ILM.

As seen from Figs. 12 and 13, as the magnetic field decreases, the equivalent anode voltage increases. So the injection ratio and the locking bandwidth decrease. Therefore, the influence of the magnetic field on the injection ratio and the locking bandwidth is also consistent with the anode voltage.

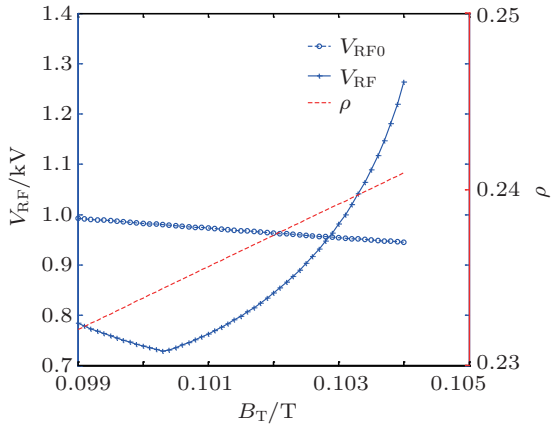


Fig. 13. (color online) Effect of the magnetic field on the RF voltage and injection ratio of ILM.

3.1. Simulation and experiment

The injection signal can significantly influence the frequency and power of the magnetron. In our laboratory, a 2.45 GHz and 15 kW high-power continuous wave magnetron is used to perform the injection-locking experiment. A 200 W injection signal within the locking range of the magnetron is injected into the magnetron. But this system can only operate at fixed voltage and magnetic field. Therefore, it cannot be directly used to validate our theory. Since the injection signal is small, it mainly plays the role of modulation. The output power and frequency of magnetron are mainly determined by the free oscillating state. Therefore, the simulation and experimental verifications of the output power and frequency are focused on FOM.

With the help of MAGIC 3D, a kind of PIC simulation software, a magnetron model with parameters in Section 3 is built. When $B_T = 0.1$ T, the magnetron's optimum operating voltage is 21 kV. Its output power is 23.5 kW and frequency is 938 MHz, which are close to our theoretical results. Therefore, by assigning reasonable parameters, the theory of this paper can give the approximate power and frequency of the magnetron.

In addition, we find that the working ranges of V_a and B_T obtained by the PIC simulation are very limited. Departing from the optimum operating point, the magnetron can hardly completely oscillate. So it is difficult to analyze the characteristics of the magnetron with variable voltage and the magnetic field by the PIC simulation. Therefore, we mainly adopt experiment data to verify the validity of the theory.

Given our experimental conditions, we only perform the experiment of FOM with a changeable magnetic field. For the variable voltage case, we adopt the experiment data of Ref. [10].

With the experimental data of Ref. [10], the power curve with the anode voltage is shown in Fig. 14. The power is approximately a quadratic function of the anode voltage. With the increase of the anode voltage, the power and its growth rate increase. So the experimental data are in good agreement with the theoretical result.

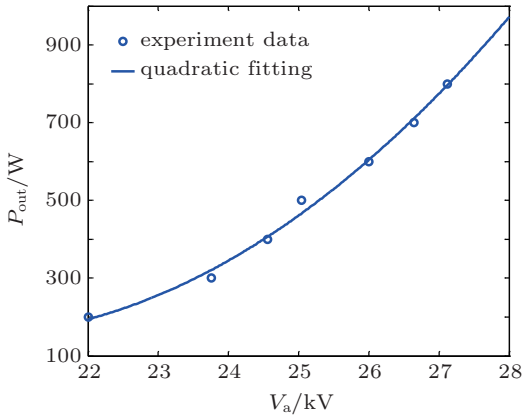


Fig. 14. (color online) Experiment data of power vs. anode voltage.

In addition, a typical frequency characteristic curve in Ref. [10] shows that, before the saturation point, the frequency increases with increasing current and the growth rate becomes slow, as shown in Fig. 15. Thus, the theoretical analysis is in agreement with the typical experimental result.

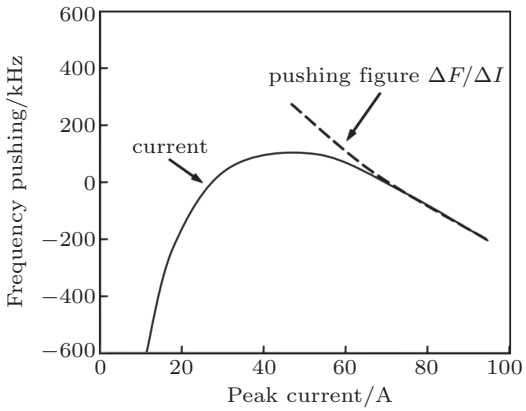


Fig. 15. Typical frequency characteristic curve.

A 20 kW and 915 MHz continuous wave magnetron is used to perform the experimental measurement with a variable magnetic field. When the anode voltage is 11.2 kV, trends of the output power and frequency with the magnetic field are shown in Figs. 16 and 17, respectively.

The experimental results in Fig. 16 show that, with the decrease of the magnetic field, the power and its growth rate increase. Similarly, as shown in Fig. 17, with the decrease of the magnetic field, the pushing effect weakens. The frequency increases, but its growth rate decreases. Therefore, the theory results are consistent with the experimental results and the typical frequency curve.

Note that the theoretical results do not completely agree with the experimental data and the simulation results. This is because the parameters adopted by the theoretical calculation are different from the actual ones. What is more, some

approximate conclusions and statistical regularities adopted in the theoretical analysis cannot describe the actual oscillating process accurately.

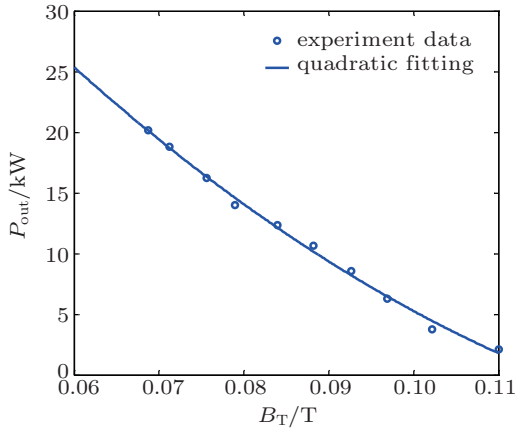


Fig. 16. (color online) Experimental results of power vs. magnetic field.

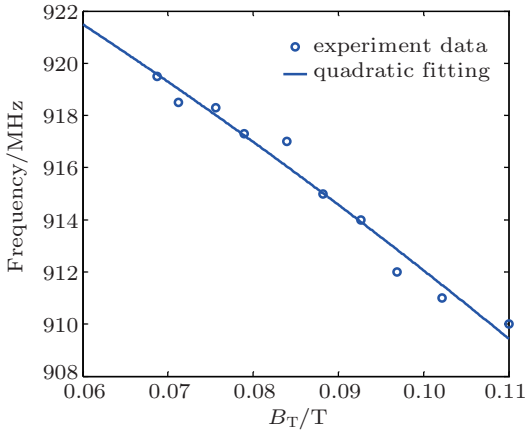


Fig. 17. (color online) Experimental results of frequency vs. magnetic field.

4. Conclusion and perspectives

The frequency characteristics of FOM and ILM are investigated. With the equivalent circuit method, the expressions of the RF voltage and frequency of FOM, as well as the locking bandwidth of ILM, on the anode voltage and magnetic field are derived. Then the frequency characteristics of the magnetron can be theoretically calculated with its anode voltage and magnetic field. The theoretical calculation results show that, with the increasing anode voltage and decreasing magnetic field, the output power and frequency of FOM increase, and the injection ratio and locking bandwidth of ILM decrease, which are consistent with the experiment results. The theory in this paper provides a theoretical guidance for the injection-locked system with variable anode voltage and magnetic field. In addition, after replacing an adjustable voltage and magnetic field power supply, the injection-locked magnetron experiment will be performed and the numerical results need further verification.

References

[1] Belanger J M, Jocelyn P J R, Poon O, Fairbridge C, Ng S, Mutyala S and Hawkins R 2008 *J. Microwave Power E. E.* **42** 24
[2] Adler R 1946 *Proc. IRE* **34** 351
[3] Pengvanich P, Neculaes V B, Lau Y Y, Gilgenbach R M, Jones M, White W M and Kowalczyk R D 2005 *J. Appl. Phys.* **98** 114903
[4] Razavi B 2004 *IEEE Journal of Solid-State Circuits* **39** 1415
[5] Zhu X Y, Jen L, Liu Q X and Du X S 1996 *Rev. Sci. Instrum.* **67** 2010
[6] Treado T A, Brown P D, Hansen T A and Aiguier D J 1994 *IEEE Trans. Plasma Sci.* **22** 616
[7] Sze H, Smith R R, Benford J N and Harteneck B D 1992 *IEEE Trans. Electromagn. Compat.* **34** 235
[8] Benford J, Sze H, Woo W, Smith R R and Harteneck B 1989 *Phys. Rev. Lett.* **62** 8
[9] Kazakevich G M, Pavlov V M, Jeong Y U and Lee B C 2011 *Nuclear Instruments and Methods in Physics Research Section A: Accelerators, Spectrometers, Detectors and Associated Equipment* **647** 10
[10] Gilmour A S 2011 *Klystrons, Traveling Wave Tubes, Magnetrons, Crossed-field Amplifiers, and Gyrotrons* (New York: Artech House) p. 523
[11] Slater J C 1947 *MIT. Cambridge, MA, RLE Tech. Rep.* **3** 1
[12] Slater J C 1946 *Rev. Mod. Phys.* **18** 489
[13] Welch Jr H W 1953 *Proc. IRE* **41** 1631
[14] David E E 1961 *Crossed Field Microwave Devices* (Vol. 2) (New York: Academic Press) p. 375
[15] David E E 1952 *Proc. IRE* **40** 669
[16] Woo W, Benford J, Fittinghoff D, Harteneck B, Price D, Smith R and Sze H 1989 *J. Appl. Phys.* **65** 861
[17] Chen S C 1990 *IEEE Trans. Plasma Sci.* **18** 570
[18] Tahir I, Dexter A and Carter R 2005 *IEEE Trans. Electron Devices* **52** 2096
[19] Tahir I, Dexter A and Carter R 2006 *IEEE Trans. Electron Devices* **53** 1721
[20] Zhou J, Liu D, Liao C and Li Z 2009 *IEEE Trans. Plasma Sci.* **37** 2002
[21] Zhang Z T 1981 *Principles of Microwave Tubes* (Beijing: National Defence Industry Press) p. 112 (in Chinese)